Adaptive fuzzy pre allocation performance control for uncertain nonlinear systems within finite time

Hai Ju *, Chenglin Li*, Xianbo Li*, Yaochun Wu **

** Anyang Product Quality Inspection and Testing Center, Anyang, 455000, Henan, China (E-mail: 253255573@qq.com)*

*** Assistant Professor, School of Mechanical and Aviation Manufacturing Engineering, Anyang Institute of Technology, Anyang, 455000, Henan, China (Corresponding author E-mail: yaochunwu@ayit.edu.cn)*

Abstract: This paper explores preassigned performance control (PPC) in finite-time for uncertain nonlinear systems under input saturation and unmeasurable states. The key is that a modified finite-time performance function is constructed such that the expected performance indicators can be obtained in finite-time. Simultaneously, the effect of saturation nonlinearity is compensated via utilizing mean-value theorem. By combining fuzzy universal approximator and adaptive parameter estimation technology, a novel PPC algorithm is developed, which realizes that tracking error converges to preassigned range in finite time. Finally, the viability of developed control algorithm is demonstrated via two examples.

Keywords: Uncertain nonlinear control, finite-time control, preassigned performance control.

1. INTRODUCTION

In practical engineering scenarios, it is critical to complete a control work as quickly as possible (Gao et al., 2024). The method of finite-time control has shown obvious advantage in realizing this target and has accordingly attracted wide attention (Sun et al., 2018; Li et al., 2022; Haddad et al., 2023; Zhang et al., 2024; Zhao et al., 2022; Zhang et al., 2024). For uncertain nonstrict systems with unknown dynamics, the authors in (Sun et al., 2018) propose practically finite-time stability criterion for the first time. On this basis, the authors in (Li et al., 2022) expand the finding from (Sun et al., 2018) to surface vehicle systems via utilizing fuzzy logic system (FLS). Moreover, for nonlinear discrete-time systems with non-vanishing uncertainties, an adaptive optimal control method is developed to realize finite-time stability (Haddad et al., 2023). By devising a matrix-weighted estimator, the authors in (Zhao et al., 2022) propose a finite-time distributed control algorithm for multi-agent systems so as to realize the leader-following formation tracking objective within finite-time.

Even so, both specific stability time and accuracy are ambiguous in above finite-time control schemes. In order to predefine expected transient and steady-state performance indicators, preassigned performance control (PPC) method, which was presented initially in (Benchlioulis et al., 2008), has garnered significant attention in recent years (Ma et al., 2022; Mao et al., 2024; Zhang et al., 2022; Chen et al., 2024; Liu et al., 2018; Fu et al., 2023). To mention a few, the authors in (Ma et al., 2022) expand the method from (Benchlioulis et al., 2008) to single-link flexible-joint robotic systems, in which an adaptive FLS control algorithm is presented to realize that tracking error converges within preassigned zone. To further optimize global performance, the authors in (Zhang et al., 2022) introduce a tuning function into the control design to alleviate the restraints on initial condition. For purpose of realizing expected performance indicators as soon as possible, a finite-time performance function (FTPF) is devised to complete the PPC objective within finite-time (Liu et al., 2018). On this basis, the authors in (Fu et al., 2023) expand the method to uncertain systems under unknown hysteresis.

In spite of this, further research is demanded to focus on the application of finite-time preassigned performance control (FTPPC) method in handling special nonlinearity characteristics, especially input saturation which attracts attention of many scholars due to its intractability and unavoidability in practical systems (Song et al., 2020; Liu et al., 2024; Li et al., 2021; Zou et al., 2024; Fotiadis et al., 2024). For switched nonlinear systems under actuator saturation, the authors in (Song et al., 2020) present a robust adaptive control scheme to ensure system stability, where an auxiliary compensation mechanism is devised to overcome the effect of saturation nonlinearity. By constructing an indicator function of saturation degree to handle asymmetric input saturation, an observer-based adaptive control algorithm is developed for switched systems with unavailable state information (Li et al., 2021). Nevertheless, these control schemes are not capable of realizing PPC in finite-time. How to develop an effective FTPPC strategy under saturation nonlinearity, is an important topic open to investigate.

Based on the above discussion, this paper explores the issue of FTPPC for uncertain systems under saturation nonlinearity and unmeasurable states. The chief contributions are outlined as follows:

(1) The developed control algorithm realizes that tracking error converges into a preassigned range in finite time. Meanwhile, both transient and steady-state performance are further optimized. Although (Liu et al., 2018) also investigate the issue of FTPPC, the unmeasurable states in this paper lead to the control algorithm in (Liu et al., 2018) unusable. By designing an observer to estimate unknown states information, the developed control scheme can be more widely applied in actual plants.

(2) Different from existing PPC strategies (Ma et al., 2022; Mao et al., 2024), the modified FTPF in the paper can complete the preassigned performance tracking control

objective with faster convergence rate. Moreover, compared to finite-time control methods (Sun et al., 2018; Li et al., 2022), both stability time and steady-state accuracy in this paper can be preassigned explicitly.

(3) This paper expands the FTPPC method from deterministic systems to uncertain systems and further takes into account the effect of saturation nonlinearity. By employing fuzzy approximate technology and devising a smooth auxiliary function, the developed control strategy not only deals with unknown dynamics but also enhances system robustness in the presence of saturation nonlinearity.

2. PRELIMINARIES AND PROBLEM FORMULATION

Lemma 1 (Zhou et al., 2024) For a continuous function $F(X_0)$ defined on compact set Θ, there is a FLS $W_0^{\mathrm{T}}\kappa_0(X_0)$ meeting

$$F(X_0)=W_0^{\mathrm{T}}\kappa_0(X_0)+\delta_0(X_0), \tag{1}$$

where $X_0\in\Theta\subset \mathrm{R}^n$, $W_0=[\omega_1,\omega_2,\ldots,\omega_N]^{\mathrm{T}}$ represents the ideal weight vector and N is the inference rules number, $\delta_0(X_0)$ represents the approximation error meeting $\|\delta_0(X_0)\|\le\varepsilon_0$, $\varepsilon_0>0$. $\kappa_0(X_0)$ and $d_i(X_0)$ are fuzzy basis function and corresponding membership functions, which can be expressed as

$$\kappa_0(X_0)=\frac{1}{\sum_{i=1}^{N}d_i(X_0)}\left[d_1(X_0),\ d_2(X_0),\ \ldots,\ d_N(X_0)\right]^{\mathrm{T}},$$

$$d_i(X_0)=\exp\left(\frac{-(X_0-y_i)^{\mathrm{T}}(X_0-y_i)}{\lambda_i^2}\right),$$

in which $y_i=\left[y_{i1},\ y_{i2},\ \ldots,\ y_{in}\right]^{\mathrm{T}}$ means the center vector, and λ_i represents the width of $d_i(X_0)$.

Lemma 2 (Fu et al., 2023) Assume that ρ_1, ρ_2, and ρ_3 are positive constants. Then for $x,y\in\mathrm{R}$, one has

$$|x|^{\rho_1}|y|^{\rho_2}\le\frac{\rho_1}{\rho_1+\rho_2}\rho_3|x|^{\rho_1+\rho_2}+\frac{\rho_2}{\rho_1+\rho_2}\rho_3^{-\frac{\rho_1}{\rho_2}}|y|^{\rho_1+\rho_2}.$$

Definition 1 (Tao et al., 2024) If a smooth function $F_p(t)$ meets: 1) $F_p(t)>0$; 2) $\dot F_p(t)<0$; 3) $\lim_{t\to T_c}F_p(t)=\hbar_{T_c}>0$ and $F_p(t)=\hbar_{T_c}$ for any $t\ge T_c$ with $\hbar_{T_c}$ denoting steady-state accuracy and T_c denoting stability time, then $F_p(t)$ is called as FTPF.

According to Definition 1, the FTPF in this paper is devised as follows

$$F_p(t)=\begin{cases}\left(\hbar_0-\dfrac{t}{T_c}\right)e^{\left(1-\frac{T_c}{T_c-t}\right)}+\hbar_{T_c} & t\in[0,T_c)\\ \hbar_{T_c} & t\in[T_c,+\infty)\end{cases}, \tag{2}$$

where $\hbar_0\ge1$ and $\hbar_{T_c}>0$ are design parameters. With the help of FTPF, both stability time and steady-state accuracy in this paper can be preassigned explicitly, thereby further increasing the convergence rate.

The controlled nonlinear system is provided as

$$\begin{cases}\dot x_i=x_{i+1}+f_i(\bar x_i) & i=1,\cdots,n-1\\ \dot x_n=u(v)+f_n(\bar x_n)\\ y=x_1\end{cases}, \tag{3}$$

where $\bar x_i=[x_1,\ldots,x_i]^{\mathrm{T}}$ denotes state vector ($x_2,\ldots,x_n$ are unmeasurable), y denotes system output, $f_i(i=1,\ldots,n)$ denotes unknown nonlinear function representing the uncertainties in the system dynamics, v represents actual control input, and $u(v)$ represents system input under saturation nonlinearity described by

$$u(v)=\begin{cases}u_M\,\mathrm{sign}(v), & |v|\ge u_M\\ v, & |v|<u_M\end{cases}, \tag{4}$$

where u_M is the bound of $u(v)$. To guarantee the system robustness under saturation nonlinearity, we construct the smooth auxiliary function as follows

$$\varpi(v)=u_M\tanh\left(\frac{v}{u_M}\right). \tag{5}$$

Then, $u(v)$ in (4) can be expressed in the following form

$$u(v)=\varpi(v)+\sigma(v), \tag{6}$$

where $\sigma(v)=u(v)-\varpi(v)$ meets

$$|\sigma(v)|=|u(v)-\varpi(v)|\le u_M\left(1-\tanh(1)\right)=\bar\sigma. \tag{7}$$

According to mean-value theorem, there is a constant τ satisfying $0<\tau<1$ so that

$$\varpi(v)=\varpi(v_0)+\varpi_{v_\tau}(v-v_0), \tag{8}$$

where $\varpi_{v_\tau}=\dfrac{\partial\varpi(v)}{\partial v}\Big|_{v=v_\tau}=\mathrm{sech}^2\left(\dfrac{v}{u_M}\right)\Big|_{v=v_\tau}$, $v_\tau=\tau v+(1-\tau)v_0$. By choosing $v_0=0$, (8) can be written as

$$\varpi(v)=\varpi_{v_\tau}v. \tag{9}$$

Assumption 1: The system (3) is input-to state stability.

According to Assumption 1, it can be found that states and control signal v in this paper are bounded. Hence, there is a positive constant ϖ_0 meeting

$$\frac{\partial\varpi(v)}{\partial v}=\mathrm{sech}^2\left(\frac{v}{u_M}\right)\ge\frac{1}{\left(e^{|v|/u_M}\right)^2}\ge\varpi_0. \tag{10}$$

The lower bound ϖ_0 will be introduced to the construction of Lyapunov function V_n in (44) later. Besides, the tracking error z_1 is defined as

$$z_1 = y - y_d , \tag{11}$$

where y_d denotes reference signal.

Assumption 2: The reference signal y_d and its time-derivatives $y_d^{(j)}$ are continuous and bounded, $j = 1, \cdots, n$.

Lemma 3 (Ioannou et al., 1996) For any bounded initial condition, if there exists a scalar function $V(x)$ meets that (i) the function $V(x)$ is continuously differentiable and positively definite; (ii) $\varpi_1(x) \le V(x) \le \varpi_2(x)$, where $\varpi_1, \varpi_2 : \mathrm{R}^n \to \mathrm{R}$ are K $-$ functions; (iii) $\dot{V} \le -\mu V + \Delta$, where μ and Δ are positive constants, then the solution of system is ultimately uniformly bounded.

The control objectives in this paper is to develop an adaptive fuzzy PPC method so that all signals in the uncertain nonlinear system are bounded and tracking error z_1 converges to preassigned range in finite time.

3. CONTROL DESIGN

3.1 Error transformation

In order to implement PPC, we define a new function $\gamma(\varsigma)$ as follows

$$\gamma(\varsigma) = \tanh(\varsigma) , \tag{12}$$

where ς means an error variable. It can be found that $\gamma(\varsigma) \in (-1,1)$, that is, $\lim_{\varsigma \to +\infty} \gamma(\varsigma) = 1$, $\lim_{\varsigma \to -\infty} \gamma(\varsigma) = -1$.

Then, the following error transformation is provided

$$z_1 = F_p(t)\gamma(\varsigma) . \tag{13}$$

Due to $\gamma(\varsigma) \in (-1,1)$ and $F_p(t) > 0$, it can be found that $-F_p(t) < F_p(t)\gamma(\varsigma) < F_p(t)$ holds. Thus, it is inferred that $-F_p(t) < z_1 < F_p(t)$, meaning that tracking error z_1 keeps within the zone $\left(-F_p(t), F_p(t)\right)$. According to the decreasing characteristic of $F_p(t)$, it can be known that z_1 converges to the set Ξ_w within a finite-time.

$$\Xi_w = \left\{ z_1 \in \mathrm{R} : |z_1| < \hbar_{T_c}, t \ge T_c \right\} . \tag{14}$$

According to (3), (11), and (13), we have

$$\begin{aligned} \dot{z}_1 &= \dot{y} - \dot{y}_d \\ &= x_2 + f_1(\bar{x}_1) - \dot{y}_d \\ &= \dot{F}_p(t)\gamma(\varsigma) + F_p(t)\frac{\partial \gamma(\varsigma)}{\partial \varsigma}\dot{\varsigma}(t) \end{aligned} . \tag{15}$$

Combining the second and third expressions in (15), one has

$$\begin{aligned} \dot{\varsigma}(t) &= \frac{x_2 + f_1(\bar{x}_1) - \dot{y}_d - \dot{F}_p(t)\gamma(\varsigma)}{F_p(t)\dfrac{\partial \gamma(\varsigma)}{\partial \varsigma}} \\ &= \mu\left(\varsigma, F_p(t)\right)\left(x_2 + f_1(\bar{x}_1) - \dot{y}_d - \phi\left(\varsigma, \dot{F}_p(t)\right)\right) \end{aligned} , \tag{16}$$

where

$$\phi\left(\varsigma, \dot{F}_p(t)\right) = \dot{F}_p(t)\gamma(\varsigma) , \tag{17}$$

$$\mu\left(\varsigma, F_p(t)\right) = \left(F_p(t)\frac{\partial \gamma(\varsigma)}{\partial \varsigma} \right)^{-1} . \tag{18}$$

Differentiating $\gamma(\varsigma)$ with respect to ς , we can obtain $\dfrac{\partial \gamma(\varsigma)}{\partial \varsigma} = \dfrac{4e^{-2\varsigma}}{\left(e^{-2\varsigma}+1\right)^2}$, meaning that $\dfrac{\partial \gamma(\varsigma)}{\partial \varsigma} > 0$ holds for any $-\infty < \varsigma < +\infty$. Furthermore, due to $F_p(t) > 0$, it can be inferred that $\mu = \left(F_p(t)\dfrac{\partial \gamma(\varsigma)}{\partial \varsigma} \right)^{-1} > 0$, which will be employed to devise the virtual control signal α_1 in (34) later.

Due to the existence of unmeasurable states in system (3), we devise the observer as

$$\begin{cases} \dot{\hat{x}}_i = \hat{x}_{i+1} + l_i\left(y - \hat{x}_1\right), \quad i = 1, \cdots, n-1 \\ \dot{\hat{x}}_n = u(v) + l_n\left(y - \hat{x}_1\right) \end{cases} , \tag{19}$$

where $\hat{x}_i$ is the estimated value of x_i , l_i is design parameter.

Let $e = \left[e_1, e_2, \ldots, e_n\right]^{\mathrm{T}}$, $\hat{x} = \left[\hat{x}_1, \hat{x}_2, \ldots, \hat{x}_n\right]^{\mathrm{T}}$, and $e = x - \hat{x}$. According to (3) and (19), one has

$$\dot{e} = A_0 e + F(x) , \tag{20}$$

where $F(x) = \left[f_1\left(\bar{x}_1\right), \ldots, f_n\left(\bar{x}_n\right) \right]^{\mathrm{T}}$, and

$$A_0 = \begin{bmatrix} -l_1 & & \\ \vdots & I_{n-1} & \\ -l_n & \cdots & 0 \end{bmatrix} . \tag{21}$$

For given positive definite matrix $Q \in \mathrm{R}^{n \times n}$, there exists positive definite matrix $P \in \mathrm{R}^{n \times n}$ meeting

$$A_0^{\mathrm{T}} P + P A_0 = -Q . \tag{22}$$

By designing the observer to estimate unknown states information, the developed control scheme can be more widely applied in actual plants.

3.2 Controller design

In this section, an adaptive fuzzy preassigned performance controller is designed by applying backstepping method, which involves n steps. The virtual errors z_i are defined as

$$z_i = \hat{x}_i - \alpha_{i-1}, \quad i = 2, \ldots, n , \tag{23}$$

where α_{i-1} represents virtual controller designed in (34) and (41) later. In each step of the backstepping method, the virtual controller α_i is designed to stabilize the current subsystem and eliminate the unstable cross terms left over from the previous step. Ultimately, the actual controller v is designed to ensure the stability of the entire closed-loop system.

According to (3), it can be inferred that

$$\begin{cases} \dot{z}_i = z_{i+1} + \alpha_i + l_i e_1 - \dot{\alpha}_{i-1} \\ \dot{z}_n = u(v) + l_n e_1 - \dot{\alpha}_{n-1}, \quad 2 \le i \le n-1 \end{cases}. \tag{24}$$

In each step of the backstepping method, a positive definite Lyapunov function is first constructed based on the transformed error variables. Subsequently, a virtual controller and an adaptive law are designed to guarantee the convergence of the Lyapunov function. In this process, a FLS is introduced to approximate the unknown nonlinear functions, and the adaptive estimation technique is utilized to estimate the norm of the ideal weight vector, so as to deal with the uncertain nonlinear dynamics.

Step 1: Choose the Lyapunov function as

$$V_1 = e^{\mathrm{T}} P e + \frac{1}{2}\varsigma^2 + \frac{1}{2g_1}\tilde{\theta}_1^2, \tag{25}$$

where $g_1 > 0$ and $\tilde{\theta}_1 = \theta_1 - \hat{\theta}_1$ with $\hat{\theta}_1$ being the estimated value of θ_1 defined in (33) later.

Differentiating V_1, one has

$$\begin{aligned} \dot{V}_1 = & -e^{\mathrm{T}} Q e + 2 e^{\mathrm{T}} P F + \varsigma\mu\left(z_2 + \alpha_1 + e_2 + f_1 - \dot{y}_d - \phi\right) \\ & - \frac{1}{g_1}\tilde{\theta}_1\dot{\hat{\theta}}_1 \end{aligned}. \tag{26}$$

Due to $F(x) = \left[f_1(\bar{x}_1), \ldots, f_n(\bar{x}_n)\right]^{\mathrm{T}}$, and $f_i(\bar{x}_i)$ is unknown, by utilizing Lemma 1, one obtains

$$f_i(X_0) = W_{i0}^{\mathrm{T}}\kappa_0(X_0) + \delta_{i0}(X_0), \quad \left\|\delta_{i0}(X_0)\right\| \le \varepsilon_{i0}, \tag{27}$$

where $X_0 = \bar{x}_i$. Therefore, one gets

$$F(X_0) = W_0^{\mathrm{T}}\kappa_0(X_0) + \delta_0(X_0), \quad \left\|\delta_0(X_0)\right\| \le \varepsilon_0, \tag{28}$$

where $W_0 = \left[W_{10}, \ldots, W_{n0}\right]^{\mathrm{T}}$, $\delta_0(X_0) = \left[\delta_{10}(X_0), \ldots, \delta_{n0}(X_0)\right]^{\mathrm{T}}$, $\varepsilon_0 = \sqrt{\varepsilon_{10}^2 + \ldots + \varepsilon_{n0}^2}$. Thus, according to Lemma 2, one has

$$\begin{aligned} 2e^{\mathrm{T}} P F &= 2e^{\mathrm{T}} P\left(W_0^{\mathrm{T}}\kappa_0(X_0) + \delta_0(X_0)\right) \\ &\le \|e\|^2 + \|P\|^2 \theta + \|P\|^2 \varepsilon_0^2 \end{aligned}, \tag{29}$$

where $\theta = \|W_0\|^2$.

According to fundamental inequality $ab \le \frac{a^2}{2} + \frac{b^2}{2}$, one gets

$$\varsigma\mu e_2 \le \frac{1}{2}\left(\varsigma\mu\right)^2 + \frac{1}{2}\|e\|^2. \tag{30}$$

Substituting (29) and (30) into (26), it can be obtained that

$$\begin{aligned} \dot{V}_1 \le & -\Pi\|e\|^2 + \varsigma\left(\mu_1 + \mu\left(z_2 + \alpha_1\right)\right) + \|P\|^2\theta \\ & + \|P\|^2\varepsilon_0^2 - \frac{1}{g_1}\tilde{\theta}_1\dot{\hat{\theta}}_1 \end{aligned}, \tag{31}$$

where $\Pi = -\left[\lambda_{\min}(Q) - \frac{3}{2}\right]$, $\mu_1 = \mu\left(\frac{1}{2}\varsigma\psi + f_1 - \dot{y}_d - \phi\right)$.

Since μ_1 is uncertain, based on Lemma 1, there is a FLS $W_1^{\mathrm{T}}\kappa_1$ such that

$$\mu_1 = W_1^{\mathrm{T}}\kappa_1 + \delta_1, \quad \left\|\delta_1\right\| \le \varepsilon_1, \tag{32}$$

where δ_1 denotes approximation error, ε_1 denotes approximation accuracy. According to Lemma 2 and taking $x = 1$, $y = \varsigma W_1^{\mathrm{T}}\kappa_1$, $\rho_1 = 1$, $\rho_2 = 1$, and $\rho_3 = a_1^2$ into account, one has

$$\begin{aligned} \varsigma\mu_1 &= \varsigma W_1^{\mathrm{T}}\kappa_1 + \varsigma\delta_1 \\ &\le \frac{1}{2a_1^2}\varsigma^2\theta_1\kappa_1^{\mathrm{T}}\kappa_1 + \frac{a_1^2}{2} + \frac{\varsigma^2}{2} + \frac{1}{2}\varepsilon_1^2 \end{aligned}, \tag{33}$$

where $\theta_1 = \|W_1\|^2$ and $a_1 > 0$.

The virtual control signal α_1 and adaptive law $\dot{\hat{\theta}}_1$ are constructed as

$$\alpha_1 = -\frac{1}{\mu}\left(\frac{1}{2a_1^2}\varsigma\hat{\theta}_1\kappa_1^{\mathrm{T}}\kappa_1 + \frac{\varsigma}{2} + \psi_1\varsigma\right), \tag{34}$$

$$\dot{\hat{\theta}}_1 = \frac{g_1}{2a_1^2}\varsigma^2\kappa_1^{\mathrm{T}}\kappa_1 - \vartheta_1\hat{\theta}_1, \tag{35}$$

where ψ_1, $\vartheta_1 > 0$.

Substituting (33)-(35) into (31), one obtains

$$\dot{V}_1 \le -\Pi\|e\|^2 + \Delta_1 + \mu\varsigma z_2 - \psi_1\varsigma^2 + \frac{\vartheta_1}{g_1}\tilde{\theta}_1\hat{\theta}_1, \tag{36}$$

where $\Delta_1 = \|P\|^2\theta + \|P\|^2\varepsilon_0^2 + \frac{a_1^2}{2} + \frac{1}{2}\varepsilon_1^2$.

Step *j* $\left(2 \le j \le n-1\right)$: Choose the Lyapunov function as

$$V_j = V_{j-1} + \frac{1}{2}z_j^2 + \frac{1}{2g_j}\tilde{\theta}_j^2, \tag{37}$$

where $g_j > 0$ and $\tilde{\theta}_j = \theta_j - \hat{\theta}_j$ with $\hat{\theta}_j$ being the estimated value of θ_j defined in (40) later.

Differentiating V_j, one gets

$$\begin{aligned}\dot{V}_j \le & -\Pi\|e\|^2 + z_j\left(\mu_j + z_{j+1} + \alpha_j\right) - \sum_{i=2}^{j-1}\psi_i z_i^2 \\ & + \sum_{i=2}^{j-1}\left(\frac{a_i^2}{2} + \frac{\varepsilon_i^2}{2}\right) + \Delta_{j-1} - \psi_1\varsigma^2 + \sum_{i=1}^{j-1}\frac{\vartheta_i}{g_i}\tilde{\theta}_i\hat{\theta}_i \,, \\ & - \frac{1}{g_j}\tilde{\theta}_j\dot{\hat{\theta}}_j\end{aligned} \tag{38}$$

where $\mu_j = z_{j-1} + l_j e_1 - \dot{\alpha}_{j-1}$. Since μ_j is uncertain, based on Lemma 1, one gets

$$\mu_j = W_j^{\mathrm{T}}\kappa_j + \delta_j, \quad \|\delta_j\| \le \varepsilon_j, \tag{39}$$

where δ_j denotes approximation error, ε_j denotes approximation accuracy. According to Lemma 2 and taking $x = 1$, $y = z_j W_j^{\mathrm{T}}\kappa_j$, $\rho_1 = 1$, $\rho_2 = 1$, and $\rho_3 = a_j^2$ into account, one has

$$\begin{aligned} z_j\mu_j &= z_j W_j^{\mathrm{T}}\kappa_j + z_j\delta_j \\ &\le \frac{1}{2a_j^2}z_j^2\theta_j\kappa_j^{\mathrm{T}}\kappa_j + \frac{a_j^2}{2} + \frac{z_j^2}{2} + \frac{1}{2}\varepsilon_j^2, \end{aligned} \tag{40}$$

where $\theta_j = \|W_j\|^2$ and $a_j > 0$.

The virtual control signal α_j and adaptive law $\dot{\hat{\theta}}_j$ are constructed as

$$\alpha_j = -\left(\frac{1}{2a_j^2}z_j\hat{\theta}_j\kappa_j^{\mathrm{T}}\kappa_j + \frac{z_j}{2} + \psi_j z_j\right), \tag{41}$$

$$\dot{\hat{\theta}}_j = \frac{g_j}{2a_j^2}z_j^2\kappa_j^{\mathrm{T}}\kappa_j - \vartheta_j\hat{\theta}_j, \tag{42}$$

where $\psi_j,\ \vartheta_j > 0$.

Substituting (40)-(42) into (38), we have

$$\dot{V}_j \le -\Pi\|e\|^2 + z_j z_{j+1} + \Delta_j - \psi_1\varsigma^2 - \sum_{i=2}^{j}\psi_i z_i^2 + \sum_{i=1}^{j}\frac{\vartheta_i}{g_i}\tilde{\theta}_i\hat{\theta}_i \,, \tag{43}$$

where $\Delta_j = \Delta_{j-1} + \frac{a_j^2}{2} + \frac{1}{2}\varepsilon_j^2$.

Step *n*: Choose the Lyapunov function as

$$V_n = V_{n-1} + \frac{1}{2}z_n^2 + \frac{\varpi_0}{2g_n}\tilde{\theta}_n^2, \tag{44}$$

where $g_n > 0$ and $\tilde{\theta}_n = \theta_n - \hat{\theta}_n$ with $\hat{\theta}_n$ being the estimated value of θ_n defined in (49) later.

Differentiating V_n, one gets

$$\begin{aligned}\dot{V}_n \le & -\Pi\|e\|^2 + z_n\left(z_{n-1} + \sigma(v) + \varpi_{v_\tau}v + l_n e_1 - \dot{\alpha}_{n-1}\right) - \\ & \sum_{i=2}^{n-1}\psi_i z_i^2 + \Delta_{n-1} - \psi_1\varsigma^2 + \sum_{i=1}^{n-1}\frac{\vartheta_i}{g_i}\tilde{\theta}_i\hat{\theta}_i - \frac{\varpi_0}{g_n}\tilde{\theta}_n\dot{\hat{\theta}}_n \end{aligned} \,. \tag{45}$$

Based on (7) and the fundamental inequality $ab \le \frac{a^2}{2} + \frac{b^2}{2}$, one has

$$z_n\sigma(v) \le \frac{1}{2}z_n^2 + \frac{1}{2}\bar{\sigma}^2. \tag{46}$$

Substituting (46) into (45), one gets

$$\begin{aligned}\dot{V}_n \le & -\Pi\|e\|^2 + z_n\left(\mu_n + \varpi_{v_\tau}v\right) - \sum_{i=2}^{n-1}\psi_i z_i^2 + \Delta_{n-1} \\ & - \psi_1\varsigma^2 + \sum_{i=1}^{n-1}\frac{\vartheta_i}{g_i}\tilde{\theta}_i\hat{\theta}_i - \frac{\varpi_0}{g_n}\tilde{\theta}_n\dot{\hat{\theta}}_n + \frac{1}{2}\bar{\sigma}^2 \end{aligned} \,, \tag{47}$$

where $\mu_n = z_{n-1} + l_n e_1 - \dot{\alpha}_{n-1} + \frac{1}{2}z_n$. Since μ_n is uncertain, based on Lemma 1, there is a FLS $W_n^{\mathrm{T}}\kappa_n$ such that

$$\mu_n = W_n^{\mathrm{T}}\kappa_n + \delta_n, \quad \|\delta_n\| \le \varepsilon_n, \tag{48}$$

where δ_n denotes approximation error, ε_n denotes approximation accuracy. According to Lemma 2 and taking $x = 1$, $y = z_n W_n^{\mathrm{T}}\kappa_n$, $\rho_1 = 1$, $\rho_2 = 1$, and $\rho_3 = a_n^2$ into account, one has

$$\begin{aligned} z_n\mu_n &= z_n W_n^{\mathrm{T}}\kappa_n + z_n\delta_n \\ &\le \frac{\varpi_0}{2a_n^2}z_n^2\theta_n\kappa_n^{\mathrm{T}}\kappa_n + \frac{a_n^2}{2\varpi_0} + \frac{\varpi_0 z_n^2}{2} + \frac{1}{2\varpi_0}\varepsilon_n^2, \end{aligned} \tag{49}$$

where $\theta_n = \|W_n\|^2$ and $a_n > 0$.

The actual control signal v and adaptive law $\dot{\hat{\theta}}_n$ are constructed as

$$v = -\left(\frac{1}{2a_n^2}z_n\hat{\theta}_n\kappa_n^{\mathrm{T}}\kappa_n + \frac{z_n}{2} + \psi_n z_n\right), \tag{50}$$

$$\dot{\hat{\theta}}_n = \frac{g_n}{2a_n^2}z_n^2\kappa_n^{\mathrm{T}}\kappa_n - \vartheta_n\hat{\theta}_n, \tag{51}$$

where $\psi_n,\ \vartheta_n > 0$.

According to (10) and (50), one gets

$$z_n\varpi_{v_\tau}v \le -\left(\frac{\varpi_0}{2a_n^2}z_n^2\hat{\theta}_n\kappa_n^{\mathrm{T}}\kappa_n + \frac{\varpi_0 z_n^2}{2} + \beta_n\varpi_0 z_n^2\right). \tag{52}$$

Substituting (49)-(52) into (47), one gets

$$\begin{aligned}\dot{V}_n \le & -\Pi\|e\|^2 + \Delta_n - \psi_1\varsigma^2 - \sum_{i=2}^{n-1}\psi_i z_i^2 + \\ & \sum_{i=1}^{n-1}\frac{\vartheta_i}{g_i}\tilde{\theta}_i\hat{\theta}_i - \psi_n\varpi_0 z_n^2 + \frac{\varpi_0\vartheta_n}{g_n}\tilde{\theta}_n\hat{\theta}_n \end{aligned} \,, \tag{53}$$

where $\Delta_n = \Delta_{n-1} + \frac{a_n^2}{2\varpi_0} + \frac{\varepsilon_n^2}{2\varpi_0} + \frac{1}{2}\bar{\sigma}^2$.

The design procedure of the controller is demonstrated from the flow chart of the control system illustrated in Fig. 1. It can be found that the control performance of the system is dependent on many design parameters. In the "State observer" block, the observer parameter l_i should be selected such that the matrix A_0 in (20) is strict Hurwitz, thereby guaranteeing the ideal observer accuracy. In the "Virtual controller" and "Actual controller" blocks, the values of ψ_i should be chosen larger and a_i should be chosen smaller, so as to increase the tracking speed and reduce the steady-state error. In the "Adaptive law" block, the values of g_i and ϑ_i should be chosen larger to improve the parameter update rate.

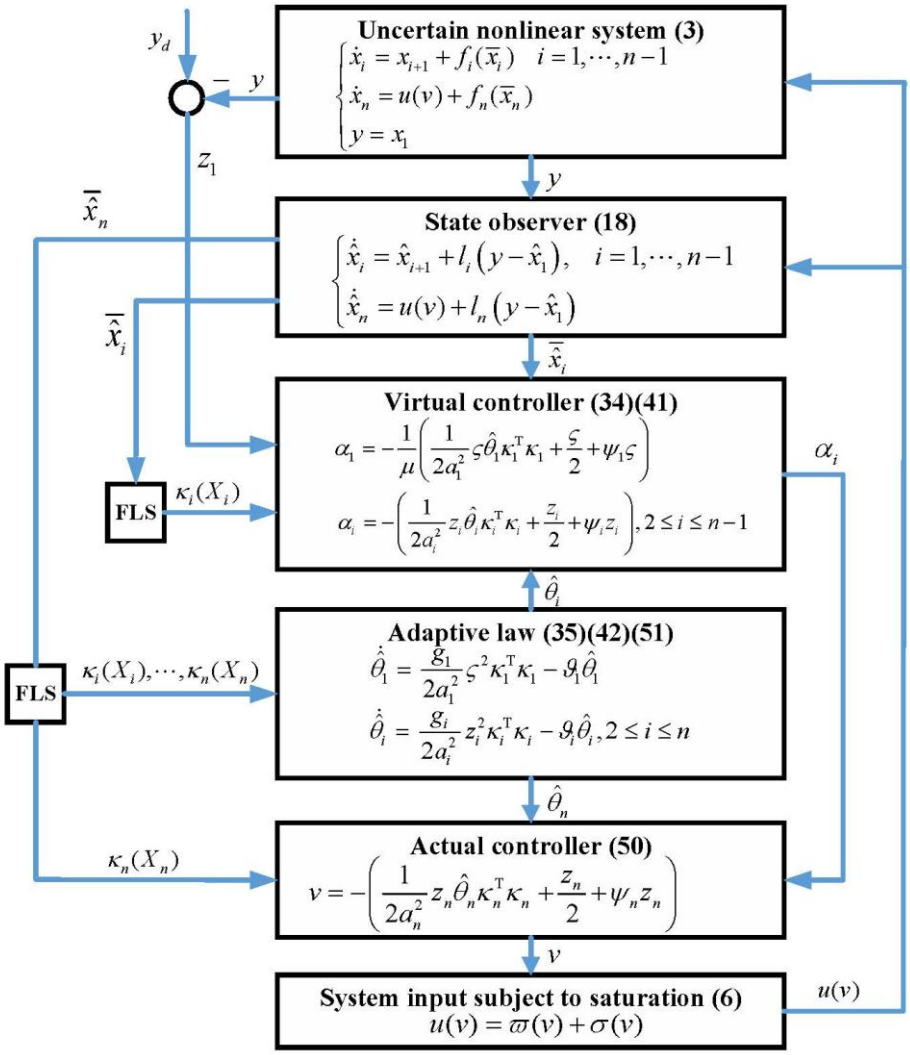

Fig. 1. Block diagram of control system.

4. STABILITY ANALYSIS

Theorem 1: For system (3) which fulfills Assumption 1, by combining fuzzy approximate technology with adaptive estimation algorithm, the designed actual control signal (50) can realize that all signals are bounded and tracking error converges to preassigned range in a finite time.

Proof: Based on $\tilde{\theta}_i = \theta_i - \hat{\theta}_i$ and the fundamental inequality $ab \le \frac{a^2}{2} + \frac{b^2}{2}$, it is inferred that

$$\frac{\vartheta_i}{g_i}\tilde{\theta}_i\hat{\theta}_i \le -\frac{\vartheta_i}{2g_i}\tilde{\theta}_i^2 + \frac{\vartheta_i}{2g_i}\theta_i^2. \tag{54}$$

Substituting (54) into (53), one has

$$\begin{aligned}\dot{V}_n &\le -\tau e^{\mathrm{T}}\mathrm{P}e + \Delta_n - \psi_1\varsigma^2 - \sum_{i=2}^{n-1}\psi_i z_i^2 + \sum_{i=1}^{n-1}\frac{\vartheta_i}{2g_i}\theta_i^2 \\ &\quad - \psi_n\varpi_0 z_n^2 + \frac{\varpi_0\vartheta_n}{2g_n}\theta_n^2 - \sum_{i=1}^{n-1}\frac{\vartheta_i}{2g_i}\tilde{\theta}_i^2 - \frac{\varpi_0\vartheta_n}{2g_n}\tilde{\theta}_n^2 \\ &\le -\bar{\gamma}_1(e^{\mathrm{T}}\mathrm{P}e + \frac{1}{2}\varsigma^2 + \sum_{i=2}^{n-1}\frac{1}{2}z_i^2 + \sum_{i=1}^{n-1}\frac{1}{2g_i}\tilde{\theta}_i^2 + \\ &\quad \frac{\varpi_0}{2g_n}\tilde{\theta}_n^2) + \sum_{i=1}^{n-1}\frac{\vartheta_i}{2g_i}\theta_i^2 + \frac{\varpi_0\vartheta_n}{2g_n}\theta_n^2 + \Delta_n \\ &\le -\bar{\gamma}_1 V_n + \bar{\gamma}_2\end{aligned}, \tag{55}$$

where $\tau = \frac{\Pi}{\lambda_{\max}(P)}$, $\bar{\gamma}_1 = \min\{\tau,\ 2\psi_1,\ \ldots,\ 2\psi_{n-1},\ 2\psi_n\varpi_0, \vartheta_1,\ \ldots,\ \vartheta_n\}$, and $\bar{\gamma}_2 = \Delta_n + \sum_{i=1}^{n-1}\frac{\vartheta_i}{2g_i}\theta_i^2 + \frac{\varpi_0\vartheta_n}{2g_n}\theta_n^2$.

According to Lemma 3, it can be known that the solution of system (3) is ultimately uniformly bounded. By integrating both sides of the inequality (55) on $[0,t]$, one gets

$$V_n \le \frac{\bar{\gamma}_2}{\bar{\gamma}_1}(1-e^{-\bar{\gamma}_1 t}) + V_n(0)e^{-\bar{\gamma}_1 t} \le \frac{\bar{\gamma}_2}{\bar{\gamma}_1} + V_n(0)e^{-\bar{\gamma}_1 t}. \tag{56}$$

Then, it is inferred that all signals in the system (3) are bounded. Furthermore, tracking error always keeps in the region $\left(-F_p(t), F_p(t)\right)$, which means that tracking error converges into preassigned range in a finite time.

5. SIMULATION EXAMPLES

Example 1: Consider the following uncertain system under saturation nonlinearity, which fulfills Assumption 1.

$$\begin{cases} \dot{x}_1 = x_2 + x_1 + \sin\left(2.2x_1^2\right) + 1 \\ \dot{x}_2 = u(v) + \cos\left(x_2^2\right) + x_1^2 \\ y = x_1 \end{cases}. \tag{57}$$

The saturation bound in (4) is chosen as $u_M = 13$, and reference signal is $y_d = 0.55\sin\left(0.533\left(t - 0.43\pi\right)\right)$.

The observer, virtual control signals, adaptive laws, and actual control signal are selected as

$$\begin{cases} \dot{\hat{x}}_1 = \hat{x}_2 + l_1\left(y - \hat{x}_1\right), \\ \dot{\hat{x}}_2 = u(v) + l_2\left(y - \hat{x}_1\right) \end{cases}, \tag{58}$$

$$\alpha_1 = -\frac{1}{\mu}\left(\frac{1}{2a_1^2}\varsigma\hat{\theta}_1\kappa_1^{\mathrm{T}}\kappa_1 + \frac{\varsigma}{2} + \psi_1\varsigma\right), \tag{59}$$

$$\dot{\hat{\theta}}_1 = \frac{g_1}{2a_1^2}\varsigma^2\kappa_1^{\mathrm{T}}\kappa_1 - \vartheta_1\hat{\theta}_1, \tag{60}$$

$$\dot{\hat{\theta}}_2 = \frac{g_2}{2a_2^2}z_2^2\kappa_2^{\mathrm{T}}\kappa_2 - \vartheta_2\hat{\theta}_2, \tag{61}$$

$$v = -\left(\frac{1}{2a_2^2}z_2\hat{\theta}_2\kappa_2^{\mathrm{T}}\kappa_2 + \frac{z_2}{2} + \psi_2 z_2\right), \tag{62}$$

where $l_1 = 100.1$, $l_2 = 100.6$, $a_1 = 0.05$, $a_2 = 0.6$, $\psi_1 = 30$, $\psi_2 = 60$, $g_1 = 20$, $g_2 = 30$, $\vartheta_1 = 0.3$, $\vartheta_2 = 33$. The initial values are selected as $x_1(0) = -0.5$, $x_2(0) = -0.2$, $\hat{\theta}_1(0) = 0$, $\hat{\theta}_2(0) = 0$, $\hat{x}_1(0) = 0$, $\hat{x}_2(0) = 0$. The parameters of FTPF in (2) are selected as $\hbar_0 = 2.5$, $\hbar_{T_c} = 0.17$, $T_c = 5$, $F_p(0) = \hbar_0 + \hbar_{T_c} = 2.67$. The fuzzy membership is defined as following:

$$d_{F_1^l}(\hat{x}_1) = \exp\frac{-(\hat{x}_1 - 3 + l)^2}{16}, \quad l = 1, \cdots, 5.$$

$$d_{F_2^l}(\hat{x}_1, \hat{x}_2) = \exp\frac{-(\hat{x}_1 - 3 + l)^2}{16} \times \exp\frac{-(\hat{x}_2 - 3 + l)^2}{16}, \quad l = 1, \cdots, 5.$$

For $\hat{x}_1$ and $\hat{x}_2$, fuzzy sets are defined over the interval $[-2,\ 2]$, and -2, -1, 0, 1, 2 are the partitioning points.

The simulation results are demonstrated in Figs. 2-6. Fig. 2 demonstrates the responses of system state x_1 and its estimated value $\hat{x}_1$, which indicates that the devised observer accurately estimates x_1. Figs. 3 and 4 demonstrate the system input u and control signal v, respectively. Fig. 5 demonstrates the tracking reference signal y_d and system output signal y. Fig. 6 demonstrates tracking error z_1 and preassigned constraints $\pm F_p$. It can be seen that the parameters T_c and $\hbar_{T_c}$ of FTPF in (2) can be adjusted to preassign the desired stability time and steady-state accuracy, respectively. Based on these results, it can be known that the developed control method is valid.

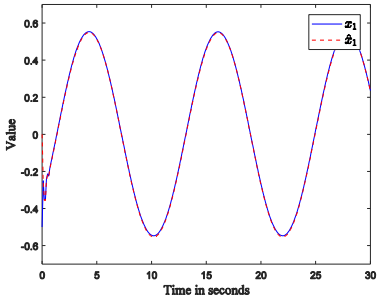

Fig. 2. The responses of x_1 and $\hat{x}_1$.

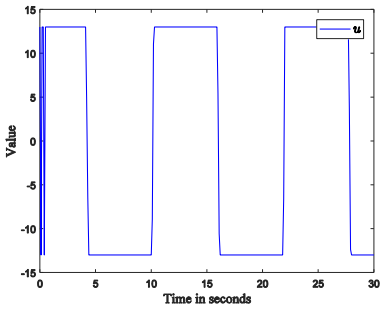

Fig. 3. The response of u.

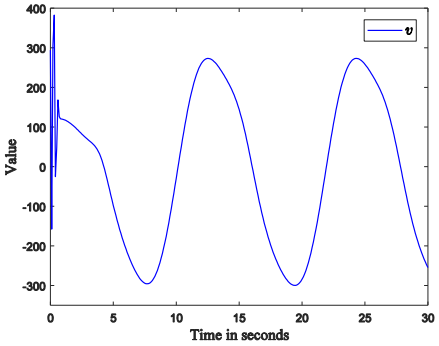

Fig. 4. The response of .

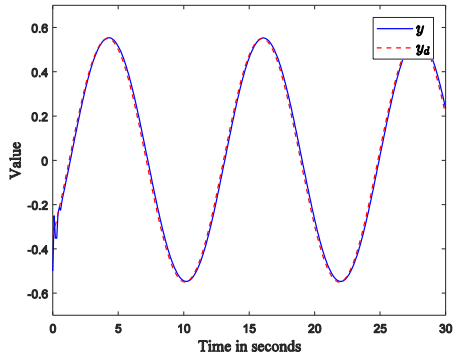

Fig. 5. The responses of y and y_d.

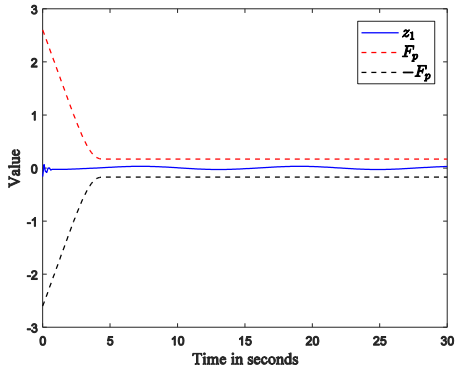

Fig. 6. The responses of z_1 and $\pm F_p$.

Example 2: The single-joint robot system (Tao et al., 2024) under saturation nonlinearity, which is illustrated in Fig. 7 and fulfills Assumption 1, is described as follows.

$$\begin{cases} \dot{x}_1 = x_2 \\ \dot{x}_2 = -\dfrac{mlg}{2G}\sin\left(x_1\right) + \dfrac{1}{G}u\left(v\right) \\ y = x_1 \end{cases} \tag{63}$$

where x_1 represents the angle of joint θ, x_2 represents the angular speed of joint $\dot{\theta}$, the acceleration of gravity is $g = 9.8\text{m/s}^2$, $m = 1\text{kg}$ represents the mass of joint, $l = 1\text{m}$ represents the extent of joint, $G = 3\text{kg m}^2$ represents damping coefficient, y represents system output, v represents the control torque of joint and u represents system input under saturation nonlinearity.

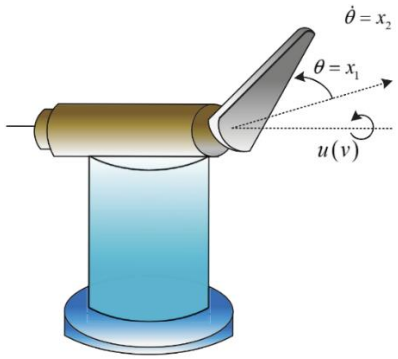

Fig. 7. A single-joint robot arm.

The reference signal is $y_d = 0.7\sin\left(2\pi\bar{f}t\right)$ with $\bar{f} = 0.08\text{Hz}$. The design parameters are chosen as $l_1 = 100.1$, $l_2 = 100.6$, $a_1 = 0.05$, $a_2 = 0.6$, $\psi_1 = 30$, $\psi_2 = 60$, $g_1 = 20$, $g_2 = 30$, $\vartheta_1 = 0.3$, $\vartheta_2 = 33$. The initial values are selected as $x_1(0) = 0.3\text{rad}$, $x_2(0) = 0.1\text{rad/s}$, $\hat{\theta}_1(0) = 0$, $\hat{\theta}_2(0) = 0$, $\hat{x}_1(0) = 0\text{rad}$, $\hat{x}_2(0) = 0\text{rad/s}$. The parameters of FTPF in (2) are selected as $\hbar_0 = 2.5$, $\hbar_{T_c} = 0.17$, $T_c = 5$, $F_p(0) = \hbar_0 + \hbar_{T_c} = 2.67$.

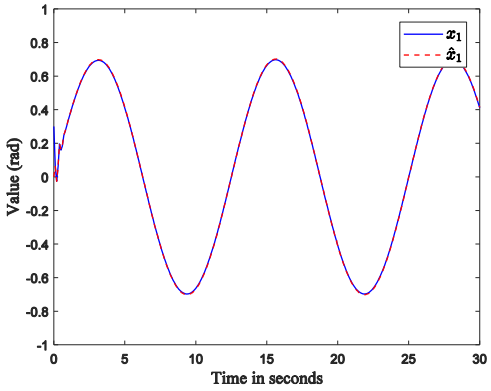

Fig. 8. The responses of x_1 and $\hat{x}_1$ of robot arm.

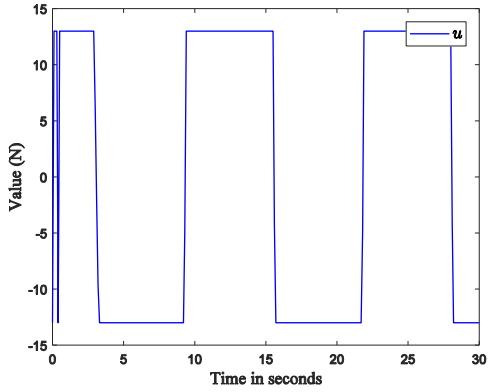

Fig. 9. The response of u of robot arm.

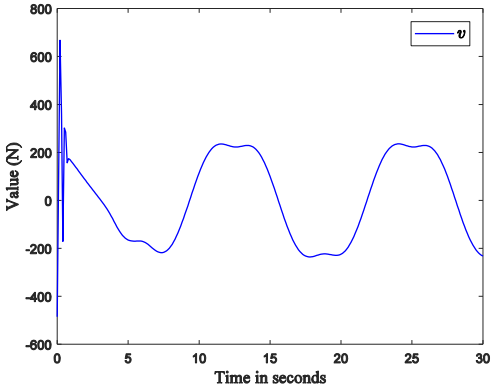

Fig. 10. The response of v of robot arm.

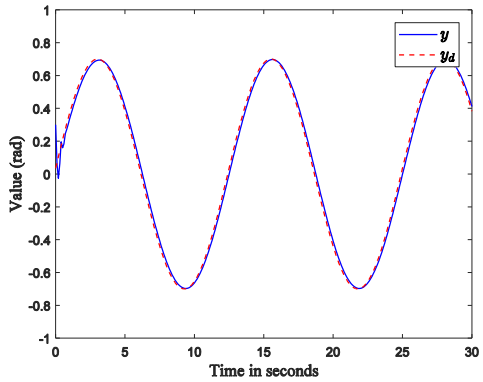

Fig. 11. The responses of y and y_d of robot arm.

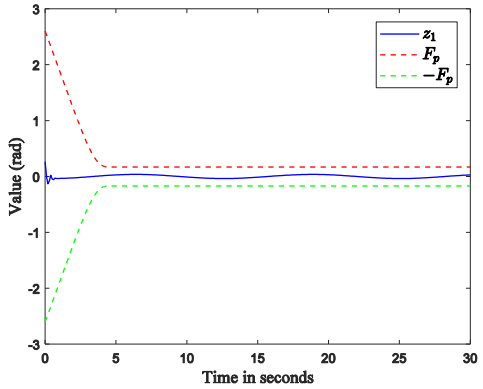

Fig. 12. The responses of z_1 and $\pm F_p$ of robot arm.

The simulation results of single-joint robot arm are demonstrated in Figs. 8-12. Fig. 8 demonstrates that the devised observer can estimate the unknown state accurately. Figs. 9 and 10 demonstrate the system input u and control torque v, respectively. Fig. 11 demonstrates the tracking reference signal y_d and system output signal y. Fig. 12 demonstrates that tracking error z_1 can converge into the preassigned constraints region $\pm F_p$.

Remark 1: The proposed control scheme offers several advantages that could be beneficial in practical applications. Firstly, it is computationally efficient, involving ordinary differential equations and inequalities that can be readily solved using standard numerical tools, making it easy to implement in actual systems. Secondly, the control strategy is designed to be robust and adaptable, with the capability to handle uncertainties and input saturation, which are common challenges in various industrial settings. Finally, the ability to achieve finite-time convergence of the tracking error within a prescribed region is particularly beneficial for applications requiring high precision and fast response, such as robotic manipulators and aerospace systems. These features collectively enhance the feasibility and applicability of the proposed approach, giving it potential application value for extension to practical scenarios.

6. CONCLUSIONS

In this paper, the problem of FTPPC for uncertain systems with unmeasurable states and input saturation is addressed. An enhanced FTPF is designed to achieve that tracking error converges into desired zone within finite-time. The proposed method is applicable to the process that can be modeled by (3). Future work will focus on extending this method to more complex systems and exploring its potential in real-world scenarios.

ACKNOWLEDGEMENTS

This work was supported by the Education Department of Henan Province of China (No: 23A460021).

REFERENCES

Benchlioulis C. and Rovithakis G. (2008). Robust adaptive control of feedback linearizable MIMO nonlinear systems with prescribed performance, *IEEE Transactions on Automatic Control*, 53(9), 2090-2099.

Chen Z., Tang J. and Zou Z. (2024). A novel prescribed-performance path-following problem for non-holonomic vehicles, *IEEE-CAA Journal of Automatica Sinica*, 11(6), 1476-1484.

Fotiadis F. and Rovithakis G. (2024). Input-constrained prescribed performance control for high-order MIMO uncertain nonlinear systems via reference modification, *IEEE Transactions on Automatic Control*, 69(5), 3301-3308.

Fu Z., Ju H., Wang N., Jiao L. and Tao F. (2023). Observer-based finite-time prescribed performance adaptive fuzzy control for nonlinear systems with hysteresis nonlinearity, *International Journal of Fuzzy Systems*, 25(6), 2397-2410.

Gao H., Wang J., Liu X. and Xia Y. (2024). Fuzzy fixed-time event-triggered consensus control for uncertain nonlinear multiagent systems with memory-based learning, *IEEE Transactions on Fuzzy Systems*, 32(6), 3682-3692.

Haddad W. and Lee J. (2023). Finite-time stabilization and optimal feedback control for nonlinear discrete-time systems, *IEEE Transactions on Automatic Control*, 68(3), 1685-1691.

Ioannou P. and Sun J. (1996). Robust Adaptive Control, *NJ: Prentice Hall.*

Li H., Zhang X. and Feng G. (2021). Event-triggered output feedback control of switched nonlinear systems with input saturation, *IEEE Transactions on Cybernetics*, 51(5), 2319-2326.

Liu W., Ma H., Liu Z., Xiong Z. and Li Y. (2024). Saturation-tolerant prescribed instant adaptive integral sliding mode control, *IEEE Transactions on Industrial Electronics*, 71(3), 3012-3023.

Liu Y., Liu X. and Jing Y. (2018). Adaptive neural networks finite-time tracking control for non-strict feedback systems via prescribed performance, *Information Sciences*, 468, 29-46.

Li Z., Xu W., Yu J., Wang C. and Cui G. (2022). Finite-time adaptive heading tracking control for surface vehicles with full state constraints, *IEEE Transactions on Circuits and Systems II: Express Briefs*, 69(3), 1134-1138.

Ma H., Zhou Q., Li H. and Lu R. (2022). Adaptive prescribed performance control of a flexible-joint robotic manipulator with dynamic uncertainties, *IEEE Transactions on Cybernetics*, 52(12), 12905-12915.

Mao B., Wu X., Liu H., Xu Y. and Lu J. (2024). Adaptive fuzzy tracking control with global prescribed-time prescribed performance for uncertain strict-feedback nonlinear systems, *IEEE Transactions on Cybernetics*, 54(9), 5217-5230.

Song Z., Li P., Wang Z., Huang X. and Liu W. (2020). Adaptive tracking control for switched uncertain nonlinear systems with input saturation and unmodeled dynamics, *IEEE Transactions on Circuits and Systems II: Express Briefs*, 67(12), 3152-3156.

Sun Y., Chen B., Lin C. and Wang H. (2018). Finite-time adaptive control for a class of nonlinear systems with nonstrict feedback structure, *IEEE Transactions on Cybernetics*, 48(10), 2774-2782.

Tao F., Ju H., Fu Z., Li M., Wang N. and Ma H. (2024). Predefined performance fuzzy control for hysteresis stochastic nonlinear systems, *International Journal of Fuzzy Systems*, 26(4), 1313-1327.

Zhang J., Wang Q. and Ding W. (2022). Global output-feedback prescribed performance control of nonlinear systems with unknown virtual control coefficients, *IEEE Transactions on Automatic Control*, 67(12), 6904-6911.

Zhang L. and Chen Y. (2024). Distributed finite-time ADP-based optimal secure control for complex interconnected systems under topology attacks, *IEEE Transactions on Systems, Man, and Cybernetics: Systems*, 54(5), 2872-2883.

Zhang Y., Wang X. and Wang Z. (2024). Discrete-time adaptive fuzzy finite-time tracking control for uncertain nonlinear systems, *IEEE Transactions on Fuzzy Systems*, 32(2), 649-659.

Zhao J., Li X., Yu X. and Wang H. (2022). Finite-time cooperative control for bearing-defined leader-following formation of multiple double-integrators, *IEEE Transactions on Cybernetics*, 52(12), 13363-13372.

Zhou H. and Tong S. (2024). Fuzzy adaptive resilient formation control for nonlinear multiagent systems subject to DoS attacks, *IEEE Transactions on Fuzzy Systems*, 32(3), 1446-1454.

Zou Y., Zou Z., Xia K. and Ding Z. (2024). Consensus of saturated multiagent systems: Tolerance to nonidentical asymmetric saturation levels, *IEEE Transactions on Automatic Control*, 69(3), 1804-1811.